

ChemComm

Accepted Manuscript



This is an *Accepted Manuscript*, which has been through the Royal Society of Chemistry peer review process and has been accepted for publication.

Accepted Manuscripts are published online shortly after acceptance, before technical editing, formatting and proof reading. Using this free service, authors can make their results available to the community, in citable form, before we publish the edited article. We will replace this *Accepted Manuscript* with the edited and formatted *Advance Article* as soon as it is available.

You can find more information about *Accepted Manuscripts* in the [Information for Authors](#).

Please note that technical editing may introduce minor changes to the text and/or graphics, which may alter content. The journal's standard [Terms & Conditions](#) and the [Ethical guidelines](#) still apply. In no event shall the Royal Society of Chemistry be held responsible for any errors or omissions in this *Accepted Manuscript* or any consequences arising from the use of any information it contains.

COMMUNICATION

AIEE Active Perylene Bisimide Supported Mercury Nanoparticles For Synthesis of Amides via Aldoximes/Ketoximes Rearrangement

Cite this: DOI: 10.1039/x0xx00000x

Sandeep Kaur, Manoj Kumar and Vandana Bhalla*

Received 00th January 2012,
Accepted 00th January 2012

DOI: 10.1039/x0xx00000x

www.rsc.org/

Aggregates of perylene bisimide (PBI) derivative 3 serve as reactors and stabilizer for the preparation of mercury nanoparticles (HgNPs) which exhibit excellent catalytic efficiency in the conversion of aldoximes/ketoximes into primary/secondary amides via Beckmann rearrangement.

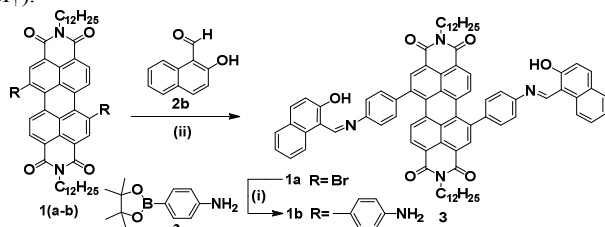
Mercury is highly toxic environmental and industrial pollutant.¹ Accumulation of mercury in the human body can affect the central nervous system, endocrine system, renal system and reproductive system.¹ Therefore, the development of new methods for the removal/detoxification of mercury is of paramount importance. For detoxification of mercury, trapping in its nano-form has been suggested as useful method.² In fact, mercury in its nano-form is more advantageous as plasmon resonance absorption of nanoparticles can be utilized in photonics and sensing.³ Despite the importance of mercury nanoparticles, there is paucity of investigations on mercury in its nano-forms. Recently, mercury nanodrops have been fabricated within PVA films which were then condensed to nanocrystals in cryo-TEM experiment.³ However, thermal annealing was needed to carry out reduction of mercury ions. Another report shows utilization of *Enterobacter sp.* strain for *in situ* generation of mercury nanoparticles (HgNPs). However, preparation of seed culture requires longer time and extensive efforts.² Thus development of a simple, fast and facile method for the generation of HgNPs is still a challenge.

Recently, from our laboratory we have reported the utilization of supramolecular assemblies of pentacenequinone and hexaphenylbenzene derivatives as reactors and stabilizer for *in situ* generation of gold, iron oxide and copper nanoparticles.⁴ However, in all these reports, except for the generation of iron oxide nanoparticles, generation of gold and copper nanoparticles was accompanied by quenching of emission intensity.⁴ The quenching probes generally have interference by fluctuations in background fluorescence resulting in low sensitivity and reliability.⁵ Therefore, preparation of fluorescent probes showing “no quenching response” is of paramount importance due to their better sensitivity and reliability.⁵ Keeping this in mind, we were

interested in the development of supramolecular aggregates which could serve as “not quenched” reactors for generation of metal nanoparticles. For this purpose, perylene bisimide (PBI) is a scaffold of our choice due to its high fluorescence quantum yield, high photostability and chemical inertness.⁶ The utilization of PBI scaffold for the preparation of fluorescent probes is scarce because of the notorious effect of aggregation-caused quenching due to its strong inter-molecular π - π stacking and attractive dipole-dipole interactions in aqueous media.⁷ To weaken the strength of inter-molecular π - π stacking, we planned to decorate PBI with bulky groups at bay positions and hence designed and synthesized perylene bisimide derivative **3** in which PBI scaffold is linked to naphthyl groups through phenyl spacer and rotatable C-C and C-N bonds. We envisaged that phenyl groups with rotatable C-C and C-N will impart aggregation induced emission enhancement (AIEE) characteristics to the molecule in the aqueous media and the presence of naphthyl groups bearing polar hydroxyl group may impart restriction to the parallel face-to-face intermolecular interactions in its aggregated state.⁸ Further, due to the presence of soft imino linkages, aggregates of derivative **3** may exhibit affinity towards mercury ions⁹ and thus could act as reactors and stabilizer for generation of HgNPs. To our pleasure, derivative **3** exhibited aggregation induced emission enhancement (AIEE) characteristics and formed fluorescent aggregates in aqueous media. Interestingly, fluorescent aggregates of derivative **3** served as reactors and stabilizer for the preparation of HgNPs and showed HgNPs mediated emission enhancement, thus, displaying “not quenched” response towards nanoparticles. Further, *in situ* generated HgNPs showed excellent catalytic efficiency in the conversion of aldoximes/ketoximes into primary/secondary amides. The work presented in this manuscript has many advantages; first, it presents a simple design for the preparation of AIEE active PBI derivative which is unprecedented. Recently, Tang *et al.* reported tetraphenylethynyl-modified perylene bisimide derivatives having aggregation induced emission enhancement characteristics (AIEE).^{7a} Their strategy of development of AIE active PBI derivative involved incorporation of

AIE active tetraphenylethenyl groups in to the PBI scaffold. In case of derivative **3**, we were successful in introducing AIEE characteristics in the molecule without having any additional AIE active unit. Second, to the best of our knowledge, this is the first report where HgNPs mediated aggregation induced emission enhancement of the PBI derivative has been demonstrated. Third, for the first time, a simple, fast, reductant free and convenient approach for development of stable HgNPs at room temperature in aqueous media has been presented and the method being reported in the present manuscript for the preparation of HgNPs is better in comparison to the other methods reported in the literature (Table S1, ESI†). Fourth, the catalytic efficiency of *in situ* generated nanoparticles in the aldoximes/ketoximes Beckmann rearrangement reaction has been demonstrated.

PBI derivative **1b** was synthesized by Suzuki-Miyaura coupling of aniline boronic ester **2a**^{9a} with **1a**¹⁰. Further, condensation of derivative **1b** with β -hydroxy naphthaldehyde, **2b** furnished derivative **3** in 86% yield (Scheme 1). The structures of derivatives **1b** and **3** were confirmed from their spectroscopic and analytical data (Fig. S26-S33, ESI†).



Scheme 1. Synthesis of PBI based derivative **3**: (i) K_2CO_3 (aq.), $\text{PdCl}_2(\text{PPh}_3)_2$, THF, 80°C ; (ii) dry THF : methanol (4 : 6), 80°C .

The fluorescence spectrum of compound **3** in THF exhibits weakly emissive band at 530 and a smaller peak at 570 nm, when excited at 485 nm (Fig. S1, ESI†).¹¹ Upon addition of water fraction up to 50% (volume fraction) to the THF solution of **3**, a slight red shift of 5 nm in the emission band at 530 nm is observed. This red shifting of the emission band is accompanied by enhancement in the emission intensity (Fig. S1, ESI†). In addition, fluorescence enhancement was also observed in the emission band at 570 nm. However, addition of more than 50% water fraction to solution of derivative **3** resulted in the decrease in fluorescence emission intensity of both the emission band (Fig. S2, ESI†). This phenomenon is often observed in derivatives with AIEE properties as after the aggregation only the molecules on the surface of aggregates emit light and contribute to the fluorescent intensity upon excitation and this leads to a decrease in emission intensity.¹² The dynamic light scattering (DLS) studies clearly show average diameter of the particles around 550 nm, 960 nm and 1400 nm in 10%, 30%, and 50% $\text{H}_2\text{O}/\text{THF}$ solvent mixture respectively (Fig. S3, ESI†). The DLS studies suggest that the aggregation driven growth is one of the reasons for the emission enhancement.¹³ The polarized optical microscopic (POM) image of the derivative **3** shows birefringence at room temperature, thus, indicating presence of ordered structure (Fig. S4(A), ESI†). The scanning electron microscopy (SEM) image of derivative **3** in $\text{H}_2\text{O}/\text{THF}$ (1:1, v/v) mixture shows the presence of interconnected rods. (Fig. S4(B), ESI†). To get insight into the AIEE phenomena, effect of variations in the viscosity and temperature on fluorescence behaviour of derivatives **3** was also investigated. The increase in fluorescence intensity of derivative **3** was

observed with increasing fraction of triethyleneglycol (TEG) (Fig. S5, ESI†). Further, the temperature dependent fluorescence spectra also showed the decrease in emission intensity with the rise in temperature from 25 to 75°C (Fig. S6, ESI†). The viscosity and temperature dependent studies suggest that restriction of intramolecular rotation (RIR) also plays a crucial role in emission enhancement of derivatives **3**.¹⁴ We also carried out time resolved fluorescence study to determine the life time of derivative **3** in the aggregated state. The time-resolved fluorescence study of derivative **3** in $\text{H}_2\text{O}/\text{THF}$ (1:1, v/v) solvent mixture (Fig. S7, ESI†) shows longer life time when monitored at 530 nm which suggests the presence of aggregated species (Table S4, ESI†). Further, the concentration dependent ^1H NMR studies of derivative **3** showed average downfield shift of 0.30 and 0.21 ppm for hydroxyl and imino protons, respectively and average upfield shift of 0.12 ppm for aromatic protons (Fig. S8, ESI†). The downfield shift of hydroxyl and imino protons suggests intermolecular hydrogen bonding between the PBI molecules. The upfield shift of aromatic protons indicates the presence of π - π interactions between the adjacent PBI molecules. On the basis of all these studies, we propose that PBI molecules form π - π stacked units which interconnect through hydrogen bonding to form closely packed fluorescent supramolecular assemblies. The dense packing arrangement of PBI molecules disfavors the structural relaxation pathways in excited state that are known for formation of non-fluorescent aggregates of PBI derivatives.¹⁵ We believe that dense packing of PBI molecules in aggregated state, aggregation driven growth of the aggregates and restriction in the intramolecular rotation of the rotors attached to the perylene core are the main reasons for the AIEE phenomena in case of derivative **3**.

The presence of imine and hydroxyl functionalities in the derivative **3** prompted us to investigate its sensing behaviour toward different metal ions (Cd^{2+} , Ba^{2+} , Hg^{2+} , Fe^{3+} , Ni^{2+} , Zn^{2+} , Cu^{2+} , Pb^{2+} , Ca^{2+} , Co^{2+} , Ag^+ , Na^+ , K^+ , Li^+ , Pd^{2+} , Cr^{3+} , and Al^{3+}) as their perchlorate/chloride/or both perchlorate and chloride salts by UV-vis and fluorescence spectroscopy in $\text{H}_2\text{O}/\text{THF}$ (1:1, v/v). Among the various metal ions tested (Fig. S9A-B, ESI†) aggregates of derivative **3** show selective response towards Hg^{2+} ions in the UV-vis spectra. Upon addition of Hg^{2+} ions (18 equiv.) to the solution of derivative **3** in mixed aqueous media ($\text{H}_2\text{O}/\text{THF}$, 1:1), two isobestic points are observed at 374 and 507 nm, respectively (Fig. S10, ESI†). Formation of these isobestic points suggests existence of more than one species in the solution. Further, a new absorption band at 290 nm corresponding to the formation of HgNPs was observed.^{3,16} (Fig. S10, ESI†). The intensity of this band increases with time (Fig. S10, ESI†). These spectral changes are accompanied by the naked eye color change from colourless to pink colour (inset, Fig. S10, ESI†). The rate constant for the formation of HgNPs was found to be $3.84 \times 10^{-3} \text{ Sec}^{-1}$ (Fig S11, ESI†). In the fluorescence spectra, upon addition of Hg^{2+} ions (0-18 equiv.) to the solution of derivative **3** ($\text{H}_2\text{O}/\text{THF}$, 1:1), fluorescence enhancement along with broadening of the spectra is observed (Fig. 1A). To rule out the possibility of hydrolysis of derivative **3** in the presence of Hg^{2+} ions, we carried out fluorescence studies of compound **1b** (one of the products in case of hydrolysis of derivative **3**) in mixed aqueous media and it was found to be non-fluorescent (Fig. S12, ESI†) while derivative **3** is highly fluorescent in presence of Hg^{2+} ions due to its AIEE characteristics (Fig. S12, ESI†). These studies clearly indicate that derivative **3** containing imine linkages do not undergo hydrolyses in the presence of Hg^{2+} ions.

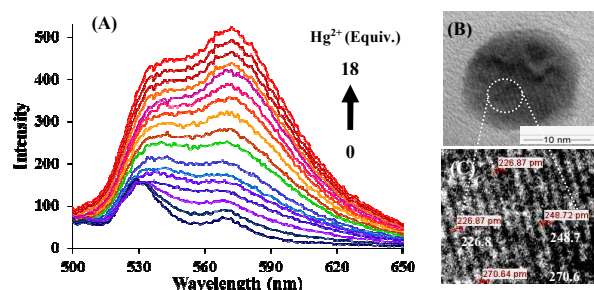


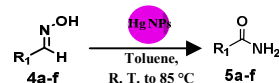
Fig. 1 (A) Fluorescence spectra of compound **3** (5 μ M) showing the response to the Hg^{2+} ion (0-18 equiv.) in $\text{H}_2\text{O}/\text{THF}$ (1:1, v/v) mixture buffered with HEPES; pH = 7.05, λ_{ex} = 485 nm. (B) TEM image of HgNPs. Scale bar 10 nm and (C) showing the interplanar spacing.

Further, the excitation spectrum of the emission at 570 nm showed peak at 309 nm which suggests that HgNPs are also contributing to the emission enhancement at 570 nm (Fig. S13, ESI \dagger).³ The changes in absorption and emission spectra suggest interaction of mercury ions with aggregates of derivative **3**, and their subsequent reduction to zero-valent mercury. The calculated detection limit was found to be 7.15 nM for Hg^{2+} ions (Fig. S14, ESI \dagger). Under the same conditions as used for Hg^{2+} ions, we also tested the binding behaviour of aggregates of derivative **3** toward other metal ions such as Cd^{2+} , Ba^{2+} , Fe^{3+} , Ni^{2+} , Zn^{2+} , Cu^{2+} , Pb^{2+} , Ca^{2+} , Co^{2+} , Ag^+ , Na^+ , K^+ , Li^+ , Pd^{2+} , Cr^{3+} , and Al^{3+} ions but no significant change in fluorescence intensity was observed (Fig. S15A-B, ESI \dagger).

We also carried out time resolved fluorescence studies of derivative **3** in the presence of mercury ions. The time-resolved fluorescence studies of derivative **3** in $\text{H}_2\text{O}/\text{THF}$ (1:1, v/v) solvent mixture in the presence of mercury ions show longer life times when monitored at 570 nm (Fig. S16, ESI \dagger). The longer life time suggests the presence of aggregated species in the presence of mercury ions (Table S5, ESI \dagger). The TEM images of aggregates of derivative **3** in the presence of mercury ions showed the presence of spherical shaped nanoparticles (Fig. 1B). It revealed the interplanar spacing³ of 2.706 Å (Fig. 1C). The DLS studies showed the formation of HgNPs having average diameter in the range of 5-20 nm (Fig. S17, ESI \dagger). The POM image of the derivative **3** containing HgNPs shows birefringence at room temperature (Fig. S18A, ESI \dagger). This study suggests the presence of aggregates having ordered morphology. Further, confocal microscopy image of compound **3** in the $\text{H}_2\text{O}/\text{THF}$ (1:1, v/v) solvent mixture in the presence of mercury ions (Fig. S18B, ESI \dagger) clearly indicates the presence of luminescent particles.

To get insight into the mechanism of formation of HgNPs, we slowly evaporated the solution of aggregates of derivative **3** containing HgNPs. After two days, precipitates were observed which were filtered and washed with THF. The ^1H NMR of the residue obtained after evaporation of THF solution showed the upfield shifting of signals corresponding to aromatic protons (Fig. S19 and Table S6, ESI \dagger). We propose that upon addition of mercury ions to the solution of aggregates of derivative **3**, the mercury ions enter the network of interconnected channels, interact with imine and hydroxyl moieties and get reduced. Thus, the aggregates of derivative **3** function as a reducing agent as well as a stabilizing agent for the preparation of HgNPs. We also carried out UV-vis studies of derivative **3** towards mercury ions in THF. However, the absorption spectrum does not indicate formation of nanoparticles (Fig. S20, ESI \dagger). These studies show the importance of

aggregates of derivative **3** for the formation of HgNPs. In the next part of our work, we were interested in investigating the catalytic efficiency of *in situ* generated HgNPs in Beckmann rearrangement for formation of amides. Amide formation reactions are one of the most important reactions in the organic chemistry due to their utility in pharmaceuticals and natural products.¹⁷ Beckmann rearrangement constitutes a fundamental tool in organic synthesis for preparation of secondary amides.¹⁸ This rearrangement, under classical conditions, requires harsh conditions such as large amount of a strong acid, high temperature, longer reaction time and is not suitable for preparation of primary amides.¹⁹ Beckmann rearrangement of aldoximes under classical reaction conditions lead to the formation of nitriles. Although some examples of transformation of aldoximes to primary amides using stoichiometric amounts of costly and very reactive reagents have been reported yet till date, development of new approaches to carry out this transformation remains a challenge. To our pleasure, in presence of *in situ* generated HgNPs, we were successful in carrying out Beckmann rearrangement reactions of aldoximes as well as ketoximes to respective amides smoothly. Transformation of various aldoximes (**4a-f**) to corresponding primary amides (**5a-f**) was carried out in the presence of *in situ* generated HgNPs (50-100 μ l, $\text{H}_2\text{O}/\text{THF}$, 1:1, v/v) in toluene (Table 1) (Scheme 2). On the other hand, the Beckmann rearrangement reactions of various ketoximes (**6a-g**) to synthesize corresponding secondary amides (**7a-g**) (Table S7, ESI \dagger) were carried out in the presence of *in situ* generated HgNPs (50 μ l, $\text{H}_2\text{O}/\text{THF}$, 1:1, v/v) in acetonitrile at room temperature (Scheme 2, ESI \dagger). The scope of rearrangement reactions of aldoximes/ketoximes was further explored by using different substrates bearing electron-donating or electron withdrawing groups at the *para*-position of the phenyl ring. The structures of all the products were characterised by their m.p., ^1H NMR and ^{13}C NMR spectra (Fig. S34-S93 in ESI \dagger). In case of aldoximes having electron donating groups at the *para*-position of the phenyl groups (**4c-d**) reactions were complete in shorter time and at room temperature whereas in other cases higher reaction time and high temperature was required. Similar trends were observed in



Scheme 2. Catalytic activity of HgNPs in synthesis of primary amides from corresponding aldoximes.

Table 1. HgNPs catalysed Beckmann rearrangement of various aldoximes to corresponding primary amides

Entry	Reactant (Aldoxime)	Product (Amide)	Temp.	Time	(%) Yield	Mp (Lit.)
1			RT	5.5h	86	125(125-127) ^{20a}
2			RT	6.5h	81	141(139) ^{20b}
3			RT	5h	93	161(165-167) ^{20a}
4			RT	5.2h	88	159(159-160) ^{20a}
5			85 °C	12h	82	196(198-200) ^{20c}
6			85 °C	10h	76	178(176-178) ^{20b}

transformation of ketoximes to secondary amides. Actually, in the presence of electrons-donating groups, phenyl ring becomes more electron rich which makes the migration faster.²¹ Additionally, it was found that *in situ* generated HgNPs could be reused upto five times in case of **6b** without significant loss of their catalytic activity (Fig S21, ESI†). We also monitored the rearrangement reactions of compounds **6b** and **6c** using *in situ* generated HgNPs by UV-visible spectra (Fig S22, 24 ESI†) and the rate constants for the formation of products **7b** and **7c** were found to be 4.96×10^{-3} and $2.19 \times 10^{-3} \text{ sec}^{-1}$ respectively (Fig S23, 25 ESI†). A plausible mechanism for the transformation of aldioximes and ketoximes to respective amides is given in schemes 3-4, ESI†.^{18,22} The efficiency of the *in situ* generated HgNPs has been tested for the rearrangement reaction of 4-methoxyacetaphenoxime (**6b**) with various amounts of catalyst, down to 10 ppm of mercury (Table S8, ESI†). When the quantities of HgNPs is 0.5 mole %, the yield is 98% in 20 min against 0% when the reaction is conducted without HgNPs. The reaction gives 80% yield when 10 ppm of HgNPs were used at room temperature during 12 h (entry 4, Table S8, ESI†). Such an extremely low quantity of catalyst has never been successfully used at room temperature for Beckmann rearrangement reactions before the present study. To the best of our knowledge, catalytic efficiency of *in situ* generated HgNPs for Beckmann rearrangement is better than that of other systems reported in literature (Table S2-S3, ESI†).

To evaluate the practical applicability of the *in situ* generated HgNPs, we also carried out the rearrangement reactions of 1,10-phenanthroline-3,8-dicarbaldehyde oxime and 2,3,4,5-tetraphenylcyclopenta-2,4-dien-1-one oxime. In both the cases, the reactions went smoothly to furnish the desired products (Scheme 5, ESI†). These studies demonstrate the practical utility of *in situ* generated HgNPs for carrying out Beckmann rearrangement reactions. In conclusion, we designed and synthesized PBI derivative **3** having naphthyl moieties which successfully overcomes the notorious effect of ACQ to exhibit AIEE behaviour and formation of fluorescent aggregates in aqueous media. The fluorescence studies of derivative **3** suggest that close packing of PBI molecules and aggregation driven-growth along with restriction of intramolecular rotation are the main causes of emission enhancement. Further, these aggregates act as reactors and stabilizer for the preparation of HgNPs and exhibit HgNPs induced emission enhancement. Moreover, the *in situ* generated nanoparticles efficiently catalysed the Beckmann rearrangement of aldioximes/ketoximes to primary/secondary amides.

We are thankful to DST, CSIR and UGC for financial support.

Notes and references: Department of Chemistry, UGC Sponsored Centre for Advanced Studies-I, Guru Nanak Dev University, Amritsar-143005, Punjab, India. E-mail: vanmanan@yahoo.co.in

†Electronic Supplementary Information (ESI) available: [Experimental details, NMR and Mass Spectra,]. See DOI: 10.1039/c000000x/

- 1 (a) J. S. Kim and D. T. Quang, *Chem. Rev.*, 2007, **107**, 3780; (b) H. N. Kim, M. H. Lee, H. J. Kim, J. S. Kim, J. Yoon, *Chem. Soc. Rev.*, 2008, **37**, 1465.
- 2 A. Sinha and S. K. Khare, *Bioresource Technology*, 2011, **102**, 4281.
- 3 G. V. Ramesh, M. D. Prasad, and T. P. Radhakrishnan, *Chem. Mater.* 2011, **23**, 5231.
- 4 (a) K. Sharma, S. Kaur, V. Bhalla, M. Kumar and A. Gupta, *J. Mater. Chem. A*, 2014, **2**, 8369; (b) S. Pramanik, V. Bhalla and M. Kumar, *Chem. Commun.*, 2014, **50**, 13533; (c) S. Kaur, V. Bhalla and M. Kumar, *Chem. Commun.*, 2015, **51**, 526.
- 5 A. Barba-Bon, A. M. Costero, S. Gil, M. Parra, J. Soto, R. Martinez-Manez and F. Sancenon, *Chem. Commun.*, 2012, **48**, 3000.
- 6 (a) F. Wurthner, *Chem. Commun.*, 2004, 1564; (b) W. Herbst, K. Hunger, *Industrial Organic Pigments*, 2nd completely revised edn.; Wiley-VCH: Weinheim, 1997.
- 7 (a) Q. Zhao, S. Zhang, Y. Liu, J. Mei, S. Chen, P. Lu, A. Qin, Y. Ma, J. Z. Sun and B. Z. Tang, *J. Mater. Chem.*, 2012, **22**, 7387; (b) Y. Che, X. Yang, K. Balakrishnan, J. Zuo and L. Zang, *Chem. Mater.*, 2009, **21**, 2930.
- 8 H. Xiao, K. Chen, D. Cui, N. Jiang, G. Yin, J. Wang and R. Wang, *New J. Chem.*, 2014, **38**, 2386.
- 9 (a) V. Bhalla, R. Tejpal, M. Kumar, R. K. Puri and R. K. Mahajan, *Tetrahedron Lett.*, 2009, **50**, 2649; (b) S. Kumari and G. S. Chauhan, *ACS Appl. Mater. Interfaces*, 2014, **6**, 5908.
- 10 Y. Huang, L. Fu, W. Zou, F. Zhang, and Z. Wei, *J. Phys. Chem. C* 2011, **115**, 10399.
- 11 Q. Dai, W. Liu, L. Zeng, C.-S. Lee, J. Wu and P. Wang, *Cryst. Eng. Comm.*, 2011, **13**, 4617.
- 12 S. Dong, Z. Li and J. Qin, *J. Phys. Chem. B*, 2009, **113**, 434.
- 13 F. Wang, M. Y. Han, K. Y. Mya, Y. Wang and Y. H. Lai, *J. Am. Chem. Soc.*, 2005, **127**, 10350.
- 14 Y. Hong, J. W. Y. Lam and B. Z. Tang, *Chem. Soc. Rev.*, 2011, **40**, 5361; (b) Y. Hong, J. W. Y. Lama and B. Z. Tang, *Chem. Commun.*, 2009, 4332.
- 15 X. Zhang, D. Gori, V. Stepanenko and F. Wurthner, *Angew. Chem. Int. Ed.*, 2014, **53**, 1270.
- 16 J. A. Creighton and D. G. Eadon, *J. Chem. Soc. Faraday Trans.*, 1991, **87**, 3881.
- 17 Polyesters and Polyamides, ed. B. L. Deopura, B. Gupta, M. Joshi and R. Alagirusami, CRC Press, BocaRaton, 2008.
- 18 C. Ramalingan and Y.-T. Park, *J. Org. Chem.*, 2007, **72**, 4536.
- 19 (a) R. E. Gawly, *Org. React.*, 1988, **35**, 1; (b) M. B. Smith and J. March, *Advanced Organic Chemistry*, 5th ed.; John Wiley & Sons: New York, 2001; p1415.
- 20 (a) A. Poeschl and D. M. Mountford, *Org. biomol. chem.*, 2014, **12**, 7150; (b) J. W. Williams, Jr. W. T. Rainay and R. S. Leopold, *J. Am. Chem. Soc.*, 1942, **64**, 1738; (c) N. A. Owston, A. J. Parker and J. M. J. Williams, *Org. Lett.*, 2007, **9**, 73.
- 21 C.-W. Kuo, M.-T. Hsieh, S. Gao, Y.-M. Shao, C.-F. Yao and K.-S. Shia, *Molecules*, 2012, **17**, 13662.
- 22 (a) R. S. Ramon, J. Bosson, S. Diez-Gonzalez, N. Marion, S. P. Nolan, *J. Org. Chem.*, 2010, **75**, 1197; (b) S. Rostammia, N. Nouruzi, H. Xin, R. Luque, *Catal. Sci. Technol.*, 2015, **5**, 199.